

REPORT DOCUMENTATION PAGE				Form Approved OMB No. 0704-0188	
Public reporting burden for this collection of information is estimated to average 1 hour per response, including the time for reviewing instructions, searching existing data sources, gathering and maintaining the data needed, and completing and reviewing this collection of information. Send comments regarding this burden estimate or any other aspect of this collection of information, including suggestions for reducing this burden to Department of Defense, Washington Headquarters Services, Directorate for Information Operations and Reports (0704-0188), 1215 Jefferson Davis Highway, Suite 1204, Arlington, VA 22202-4302. Respondents should be aware that notwithstanding any other provision of law, no person shall be subject to any penalty for failing to comply with a collection of information if it does not display a currently valid OMB control number. PLEASE DO NOT RETURN YOUR FORM TO THE ABOVE ADDRESS.					
1. REPORT DATE (DD-MM-YYYY) 29-01-2007		2. REPORT TYPE Journal Article		3. DATES COVERED (From - To)	
4. TITLE AND SUBTITLE  Chemical Reaction Modeling for Hypervelocity Collisions between O and HCl				5a. CONTRACT NUMBER	
				5b. GRANT NUMBER	
				5c. PROGRAM ELEMENT NUMBER	
6. AUTHOR(S) T. Ozawa & D.A. Levin (Penn. State Univ.); I.J. Wysong (AFRL/PRSA) (USC/Los Angeles)				5d. PROJECT NUMBER	
				5e. TASK NUMBER 50260532	
				5f. WORK UNIT NUMBER	
7. PERFORMING ORGANIZATION NAME(S) AND ADDRESS(ES)  Air Force Research Laboratory (AFMC) AFRL/PRSA 10 E. Saturn Blvd. Edwards AFB CA 93524-7680				8. PERFORMING ORGANIZATION REPORT NUMBER  AFRL-PR-ED-JA-2007-045	
9. SPONSORING / MONITORING AGENCY NAME(S) AND ADDRESS(ES)  Air Force Research Laboratory (AFMC) AFRL/PRS 5 Pollux Drive Edwards AFB CA 93524-7048				10. SPONSOR/MONITOR'S ACRONYM(S)	
				11. SPONSOR/MONITOR'S NUMBER(S) AFRL-PR-ED-JA-2007-045	
12. DISTRIBUTION / AVAILABILITY STATEMENT  Approved for public release; distribution unlimited (PA #07026A)					
13. SUPPLEMENTARY NOTES © 2007 American Institute of Physics, published in Physics of Fluids <b>19</b> , 056102 (2007).					
14. ABSTRACT  Treatment of chemical reactions in rarefied, nonequilibrium flows has been the subject of significant research. In some cases, proper treatment of reactions is needed to accurately predict overall shock thickness, stand-off, and heat transfer. In other cases, such as when reactants are minor species, the overall flowfield is not affected by details of the reaction model, but a particular radiation signature may be strongly affected. A case of the latter situation is the subject of the present study, and allows for a detailed examination of several issues important to chemical reaction models for rarefied, high-speed flows.					
15. SUBJECT TERMS					
16. SECURITY CLASSIFICATION OF:			17. LIMITATION OF ABSTRACT  SAR	18. NUMBER OF PAGES  15	19a. NAME OF RESPONSIBLE PERSON Dr. Ingrid Wysong
a. REPORT Unclassified	b. ABSTRACT Unclassified	c. THIS PAGE Unclassified			19b. TELEPHONE NUMBER (include area code) N/A

# Chemical reaction modeling for hypervelocity collisions between O and HCl

T. Ozawa<sup>a)</sup> and D. A. Levin<sup>b)</sup>

Department of Aerospace Engineering, The Pennsylvania State University, University Park, Pennsylvania 16802

I. J. Wysong<sup>c)</sup>

Air Force Research Laboratory-Space and Missile Propulsion Division, Aerophysics Branch, Edwards Air Force Base, California 93524

(Received 9 September 2006; accepted 8 February 2007; published online 10 May 2007)

The sensitivity of a rarefied-to-transitional flow to the fidelity of the chemical reaction model is investigated for a new molecular dynamics/quasiclassical trajectory (MD/QCT)-derived model and compared with the widely used total collision energy (TCE) model of Bird. For hypervelocity collisions that occur in the space environment, it is not clear, *a priori*, that the TCE model will provide reasonable results for the required high energy range and, particularly, if strong favoring of the reaction among different forms of reactant energy occurs. In fact, in previous work, the TCE model, using available Arrhenius parameters, has been found, for these flow conditions, to give unphysical probabilities. A chemical reaction model, suitable for use in the direct simulation Monte Carlo (DSMC) method, is developed to simulate the hypervelocity collisions of  $O(^3P) + HCl(^1\Sigma^+) \rightarrow OH(^2\Pi) + Cl(^2P)$ , an example of an important reaction in high-altitude atmospheric-jet interactions. The model utilizes the MD/QCT method with a new benchmark triplet  $A''$  surface. Since the modeling of chemical reactions in DSMC simulations requires the use of a reaction probability, the adequacy of the overall collision cross section, usually modeled by the variable hard sphere (VHS) model, is also considered. To obtain an accurate collision cross section, the approach of Tokumasu and Matsumoto was used in the MD/QCT method with the aforementioned potential energy surface. Energy transfer between the target HCl translational and internal energy modes was investigated and it was found that the variation of the inelastic cross section has a negligible effect on the transport cross section. Therefore, a MD/QCT VHS equivalent collision cross section was obtained and along with the MD/QCT reaction cross sections were utilized in the full DSMC calculation of the flow field. It was found that for a low enthalpy reaction, in hypervelocity collisions, the TCE model with accurate Arrhenius rates appears to agree well with the rigorous MD/QCT calculations which shows that the reaction does not exhibit strong favoring. © 2007 American Institute of Physics. [DOI: 10.1063/1.2717692]

## I. INTRODUCTION

Treatment of chemical reactions in rarefied, nonequilibrium flows has been the subject of significant research. In some cases, proper treatment of reactions is needed to accurately predict overall shock thickness, standoff, and heat transfer.<sup>1</sup> In other cases, such as when reactants are minor species, the overall flow field is not affected by details of the reaction model, but a particular radiation signature may be strongly affected.<sup>2</sup> A case of the latter situation is the subject of the present study, and allows for a detailed examination of several issues important to chemical reaction models for rarefied, high-speed flows.<sup>3,4</sup>

The most widely used method for calculating reaction probabilities in direct simulation Monte Carlo (DSMC) (Ref. 5) is the total collision energy (TCE) model.<sup>5,6</sup> Collision pairs are sampled according to the usual method, and each

pair is tested for reaction. The reaction probability is an assumed function of the total collision energy of the reactant molecules that, under equilibrium conditions, will reproduce experimental reaction rates  $K_f(T)$  in the modified Arrhenius form,

$$K_f = AT^n \exp(-E_a/kT), \quad (1)$$

where  $A$  is the pre-exponential factor,  $E_a$  is the activation energy, and  $n$  is an additional temperature dependence. In addition, the TCE model requires an input parameter defining the number of degrees of freedom of the internal energy modes of the reactants that contribute to the reaction probability.

There are two major concerns with the TCE chemistry model. First, while the assumed form of the probability reproduces measured rates under equilibrium conditions, it may not accurately describe the reaction under highly nonequilibrium conditions, especially if the reaction is activated primarily via energy in a particular mode (i.e., favoring) rather than via the total energy. Second, while literature rate

<sup>a)</sup>Electronic mail: txo123@psu.edu

<sup>b)</sup>Electronic mail: dalevin@psu.edu

<sup>c)</sup>Electronic mail: Ingrid.Wysong@edwards.af.mil

expressions (such as those to be discussed in this work) are fit to data and are valid only for a prescribed range of temperatures, high velocity flows involve collision energies that correspond to a much higher temperature range. Extrapolating Arrhenius parameters which are only valid up to 3000 K into the 10 000 K range and beyond should be avoided if at all possible. For instance, extrapolating the expression of Mahmud<sup>7</sup> (defined below) beyond 7000 K leads to reaction rates that were found in earlier work<sup>4</sup> to be higher than the total collision rate—a clearly unphysical situation. In general, the TCE model provides reasonable results if it is used with sound Arrhenius parameter values for the relevant energy range and if there is no strong favoring of the reaction among different forms of reactant energy. While one cannot criticize the use of this approach if no better information is available, it certainly motivates a search for alternatives.

The proposed approach to be discussed in this work addresses both concerns mentioned above. The molecular dynamics/quasiclassical trajectory (MD/QCT) method of computing reaction cross sections can be expected to provide reliable results over the energy range of interest, so long as the potential energy surface (PES) used is adequate and quantum mechanical effects such as tunneling are not important. The emphasis of this paper is to evaluate the adequacy of the relatively simple TCE model for the  $O+HCl \rightarrow OH+Cl$  reaction, important in high-altitude atmospheric-jet interactions. Chemical reaction probabilities obtained by the TCE method may then be tested with this more fundamental approach involving new calculations using the MD/QCT method and the recent, benchmark triplet  $A''$  PES for  $O+HCl$ .<sup>8</sup> Since the modeling of chemical reactions in DSMC simulations requires the use of a reaction probability, the adequacy of the overall collision cross section, usually modeled by the variable hard sphere (VHS) model, must also be considered. To obtain an accurate collision cross section, the approach of Tokumasu and Matsumoto<sup>9</sup> was used in the MD/QCT method with the aforementioned potential energy surface.

Energy transfer between the target HCl translational and internal energy modes was investigated and it was found that the variation of the inelastic cross section has a negligible effect on the transport cross section. Hence, MD/QCT calculations are able to predict inelastic cross sections and allow for a more accurate estimation of the viscosity and total collision cross section at high velocities. The latter is a further test of the adequacy of the VHS model which is assumed to be correct in the TCE approach.

Hypervelocity collisions such as  $O+HCl$  occur in the jet-atmospheric interaction created in the rarefied space environment when a reaction control system (RCS) is positioned on the side of a hypersonic vehicle. The large diffuse interaction region created by the rarefied, high Mach number chemically reacting flow is due to the high relative velocities of the freestream atomic oxygen and the HCl plume exhaust species. The accurate modeling of the interaction region is complicated not only by the presence of hypervelocity collisions, but also by the complex gas dynamics. The evacuation of a thruster with concentration approximately four orders of magnitude higher than the low-pressure space environment

into the diffuse wind creates a wide range of characteristic length scales in the flow. The emphasis of earlier work<sup>3,4</sup> was to establish a computational approach that insured an accurate DSMC solution, capturing the changing flow physics over the range of freestream conditions at altitudes of 80–120 km and speeds of 3–8 km/s. The bow-shock interaction region was observed to have continuum-like features for all speeds at 80 km, and the strength of the reaction region in terms of the number of chemical reactions between freestream and thruster species was found to scale with vehicle velocity, as would be expected.

In this work we propose an approach for modeling hypervelocity chemical reactions between thruster and atmospheric species in a manner suitable for DSMC simulations. Since HCl is present in high concentration in the thruster plume, and chemically reactive atomic oxygen is available as a large percentage of the freestream, accurate modeling of the  $O+HCl$  reaction at hypervelocity conditions is crucial to predicting the occurrence of OH, an important radiator. In fact, at altitudes of 120 km or higher, O exchange with HCl was found to contribute more than 70% of the OH produced.<sup>3</sup> Although other plume fragments will also exist in the flow, the comparison between TCE and *ab initio* MD/QCT calculations for  $O+HCl$  will provide an assessment of the overall feasibility of using TCE to model similar hypervelocity collisions.

The outline of the remainder of this paper is as follows: Sec. II describes some problems with using the TCE model for hypervelocity collisions in the jet-atmospheric interaction and the need for accurate high velocity collision cross sections. The MD/QCT modeling of the reaction and collision cross sections is presented in Sec. III. In Sec. IV, we discuss the specific DSMC numerical parameters used for the single freestream condition examined here: 120 km, 5 km/s. Finally, in Sec. V, we present detailed comparison of the MD/QCT results with the TCE model as well as more accurate high temperature  $O+HCl$  viscosity values and compare the changes observed in the DSMC simulation for the different chemical reaction parameters for the  $O+HCl$  reaction. Although there are multiple chemical reactions that contribute to the production of OH, we limit our discussion to the  $O+HCl$  reaction, since that is the most energetically favorable reaction path.

## II. ISSUES WITH USING THE TCE MODEL

In our previous work,<sup>3</sup> the Arrhenius parameters from Mahmud *et al.*,<sup>7</sup>  $A=5.6 \times 10^{-27}$  m<sup>3</sup>/molecule/s,  $n=2.87$ , and  $E_a=2.44 \times 10^{-20}$  J, were used for TCE calculations for the  $O+HCl \rightarrow OH+Cl$  reaction, but in this work, Arrhenius parameters based on the recent calculations of Xie *et al.*<sup>10</sup> (shown in Table I) were used and compared. The entire set of chemical reactions used in the DSMC simulations can be found in earlier work.<sup>3</sup> None of the other reactions were found to be important to the overall flow field characteristics or to the production of OH, so the TCE model was used to calculate all other reactions. A schematic of the flow geometry for the RCS plume-atmospheric interaction is given in Fig. 1. We will consider a generic RCS-vehicle geometry

TABLE I. Freestream-plume species reactions for OH production reactions used in the TCE model.

Reaction	$A, \text{m}^3/\text{s}$	$n$	$E_a, \times 10^{-19} \text{ J}$
$\text{H}_2\text{O} + \text{N}_2 \rightarrow \text{OH} + \text{H} + \text{N}_2$	$5.81 \times 10^{-15}$	0.00	7.314
$\text{H}_2\text{O} + \text{O}_2 \rightarrow \text{OH} + \text{H} + \text{O}_2$	$1.13 \times 10^{-7}$	-1.31	8.197
$\text{H}_2\text{O} + \text{O} \rightarrow \text{OH} + \text{H} + \text{O}$	$1.13 \times 10^{-7}$	-1.31	8.197
$\text{H}_2\text{O} + \text{O} \rightarrow \text{OH} + \text{OH}$	$1.13 \times 10^{-16}$	0.00	1.275
$\text{H} + \text{O}_2 \rightarrow \text{OH} + \text{O}$	$1.66 \times 10^{-16}$	0.00	1.061
$\text{O} + \text{H}_2 \rightarrow \text{OH} + \text{H}$	$3.12 \times 10^{-16}$	0.00	0.952
$\text{OH} + \text{Cl} \rightarrow \text{O} + \text{HCl}$	$3.10 \times 10^{-27}$	2.91	0.070
$\text{O} + \text{HCl} \rightarrow \text{OH} + \text{Cl}$ (Mahmud) <sup>a</sup>	$5.60 \times 10^{-27}$	2.87	0.244
$\text{O} + \text{HCl} \rightarrow \text{OH} + \text{Cl}$ (Xie) <sup>b</sup>	$1.70 \times 10^{-22}$	1.485	0.408

<sup>a</sup>Reference 7.<sup>b</sup>Reference 10.

with freestream conditions corresponding to those of high altitude, hypersonic flight for a lateral side jet thrusting perpendicular to the rocket velocity vector.

To illustrate the issues involved in the previous calculations, Fig. 2 shows the spatial distribution of the TCE reaction probability for  $\text{O} + \text{HCl} \rightarrow \text{OH} + \text{Cl}$  in the  $X$ - $Y$  plane of a sample calculation using the extrapolated Mahmud rates.<sup>7</sup> For an altitude of 120 km and a freestream velocity of 5 km/s, the typical interaction region ahead of the thruster jet is seen. It is observed that the TCE reaction probabilities for this reaction are greater than unity in the interaction region. This behavior is due to the extrapolations to much higher temperature/energy regime than that for which the Mahmud parameters are valid, as was mentioned above. If one could measure reaction rates for much higher temperatures, it is extremely unlikely that the rate coefficient would continue to increase with the same steep temperature dependence. Figure 3 shows the distribution of TCE reaction probability for all the  $\text{O} + \text{HCl} \rightarrow \text{OH} + \text{Cl}$  reactions in the entire domain, showing that more than 10% of the collisions have a reaction probability greater than unity. Since a probability greater than one has no meaning in a statistical calculation, the specific implementation used in Ref. 3 was to artificially set these probabilities equal to unity. This limit causes a smaller number of reactions to occur in the simulation compared to that predicted by the Arrhenius rate.

Another question that affects the reaction probabilities using either the TCE or MD/QCT model is the assumed value of the collision cross section. The definition of a local

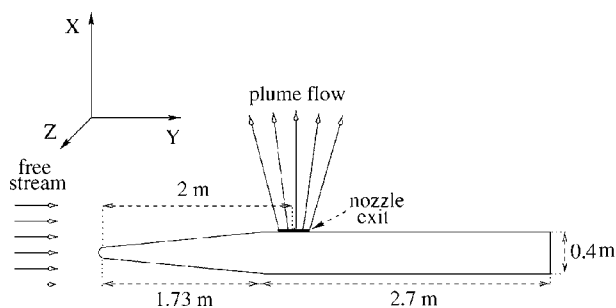
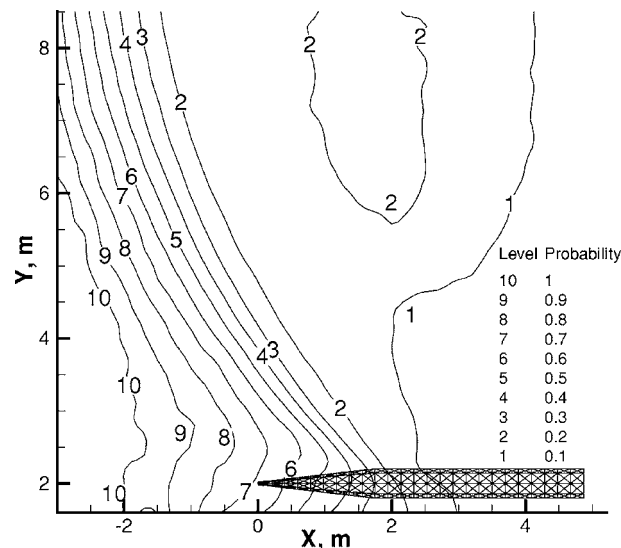
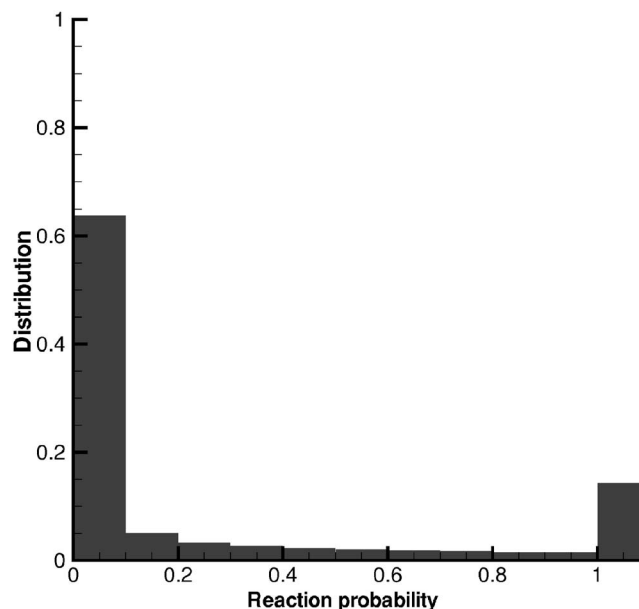


FIG. 1. Schematic of the flow.

FIG. 2. Reaction probability distribution in the  $xy$  plane for  $\text{O} + \text{HCl} \rightarrow \text{OH} + \text{Cl}$  using the TCE model (rate constant of Mahmud *et al.*, Ref. 7) for an altitude of 120 km and a freestream velocity 5 km/s.

collision frequency based on cell number density and the velocity-dependent collision cross section for any sampled pair of molecules is fundamental to the DSMC method. The collision cross section is most commonly defined by the variable hard sphere (VHS) model,<sup>6</sup> where the reference diameter and velocity-dependence are defined by parameters that reproduce a given temperature-dependence of the viscosity. There are large uncertainties in the values of the VHS model parameters, which are obtained from relatively low temperature flows, for high energies. An improved approach for obtaining appropriate high-energy VHS parameters is presented in the following section.

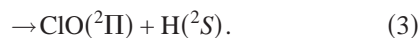
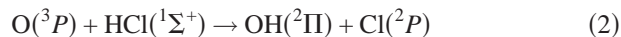
FIG. 3. Reaction probability distribution for  $\text{O} + \text{HCl} \rightarrow \text{OH} + \text{Cl}$  using the TCE model (rate constant of Mahmud *et al.*, Ref. 7) for an altitude of 120 km and a freestream velocity 5 km/s.

Since the TCE model reproduces the prescribed reaction rates (under equilibrium conditions) by definition, a different value in the VHS collision cross section does not affect the reaction rate produced in a computational cell. A lower value of VHS collision cross section, for instance, would increase the reaction probability, but then would correspondingly decrease the total number of collisions in the cell, thus producing the same overall rate of reactions. Hence, the assumed value for the VHS collision cross section will not change the number of reactions in a simulation using the TCE model. However, the collision cross section values are very important in defining the reaction probabilities resulting from the MD/QCT calculations. These probabilities are used directly as a lookup table during the DSMC simulation. In addition, comparisons between computed reaction probabilities resulting from MD/QCT and resulting from TCE will be affected by the collision cross section used.

### III. MD/QCT MODELING OF THE REACTION PROBABILITY AND COLLISION CROSS SECTION

#### A. MD/QCT reaction probability

A parallel MD/QCT code<sup>2</sup> was developed to calculate the reaction and viscosity cross sections using the QCT-internal energy quantum mechanical threshold (QCT-IEQMT) method.<sup>11</sup> For the  $\text{O}+\text{HCl} \rightarrow \text{OH}+\text{Cl}$ , the *ab initio*  $^3A''$  potential energy surface of Ramachandran and Peterson (RP) (Ref. 8) was utilized. The RP PES is accurate for total energies less than 40 kcal/mol. However, for energies higher than 40 kcal/mol, the reaction of  $\text{O}+\text{HCl}$  may have two possible outcomes,



The second channel forms the ClO system, a stable radical, but a potential for this channel is not available. Xie *et al.*<sup>10</sup> estimated the contribution from this channel and found that at 3200 K (a maximum total energy of about  $4.42 \times 10^{-19}$  J), the rate constant for this channel was roughly two orders of magnitude smaller than the total rate constant. At 120 km altitude with a freestream velocity of 5 km/s, most of the  $\text{O}+\text{HCl}$  collisions have the energy less than  $5 \times 10^{-19}$  J. Thus, in this work, we neglect this channel. The RP surface was also utilized by Xie *et al.*, who computed both quantum and QCT reaction cross sections for a range of energies.<sup>12</sup> However, it was necessary for us to perform our own MD/QCT calculations since a large set of probabilities are required for the DSMC flow field simulation, and we require cross sections for high total collision energy values. In addition, the DSMC model used here assumes that the vibrational and rotational energies are continuous, thus requiring a table of probabilities for a range of internal energies,  $E_{\text{int}}$ , while Xie *et al.* computed reaction cross sections for the vibrational quantum number,  $v=0, 1$ , and 2 states only. It will be shown in Sec. IV that the MD/QCT results presented here agree well with those of Xie *et al.* for the energy range considered in that work.<sup>12</sup>

The MD/QCT reaction probability is the ratio of the reaction cross section obtained by the QCT-IEQMT method to the total collision cross section. An efficient Monte Carlo numerical procedure is utilized to evaluate the multidimensional integrals associated with averaging of the scattering geometric properties before a collision. The Monte Carlo method converges at a rate that is independent of the dimensionality of the integral. In order to utilize the Monte Carlo method, the specific initial states of each of the trajectories that correspond to the desired reaction cross section, such as  $\sigma_r(v, J, E_{\text{tr}})$  or  $\sigma_r(E_{\text{int}}, E_{\text{tr}})$ , where  $v$  is the vibrational quantum number,  $J$  is the rotational quantum number, and  $E_{\text{tr}}$  is the translational energy, are needed. Microcanonical sampling enables one to efficiently sample the initial states of the target molecule of equal energy to obtain the trajectory initial conditions necessary to perform the MD/QCT calculations.<sup>13</sup> For the DSMC simulations, the reaction probability of a chemical reaction as a function of translational energy,  $E_{\text{tr}}$ , and molecular internal energy,  $E_{\text{int}}$ , is used. The reaction cross section,  $\sigma_r$ , is obtained by evaluating whether a  $\text{O}+\text{HCl}$  collision ends in a chemical reaction by

$$\sigma_r = \pi b_{\text{max}}^2 \frac{N_r}{N_T}, \quad (4)$$

where  $b$  is the impact parameter,  $b_{\text{max}}$  is the maximum impact parameter beyond which a chemical reaction does not occur,  $N_r$  is the number of trajectories that result in a reaction, and  $N_T$  is the number of total trajectories. In previous work,<sup>2</sup> the reaction probability,  $P_r$ , for another chemical reaction was assumed to be

$$P_r = \frac{\sigma_r}{\sigma_{\text{VHS}}}. \quad (5)$$

For the  $\text{O}+\text{HCl}$  case, however, it will be shown that the MD/QCT collision cross section is different than that given by the VHS model and will be discussed further in the next subsection.

#### B. Collision cross section

As mentioned above, in our previous work, the variable hard sphere (VHS) model with Bird values was used for the collision cross section. The VHS cross section is defined by  $\sigma_{\text{VHS}} = \pi d^2$  with<sup>6</sup>

$$d = d_{\text{ref}} \left( \frac{(2kT_{\text{ref}})^{\omega}}{(m_r g^2)^{\omega} \Gamma(2-\omega)} \right)^{1/2}, \quad (6)$$

where  $d$  is the diameter of a molecule,  $m_r$  is the molecular reduced mass,  $g$  is the relative velocity, and  $\omega$  is the viscosity index ( $\omega = \nu - 0.5$ ,  $\nu$  is the temperature exponent of the viscosity coefficient).  $\omega = 0.375$ ,  $d_{\text{ref}} = 4.38$  Å, and  $T_{\text{ref}} = 273$  K for the  $\text{O}+\text{HCl}$  reaction in Ref. 5. The reference diameters,  $d_{\text{ref}}$ , are calculated from the viscosity data,

$$d_{\text{ref}} = \left( \frac{30(mkT_{\text{ref}}/\pi)^{1/2}}{4(4-2\omega)(6-2\omega)\mu_{\text{ref}}} \right)^{1/2}, \quad (7)$$

where  $\mu_{\text{ref}}$  is the reference viscosity coefficient, and  $m$  is the mass of the molecule.



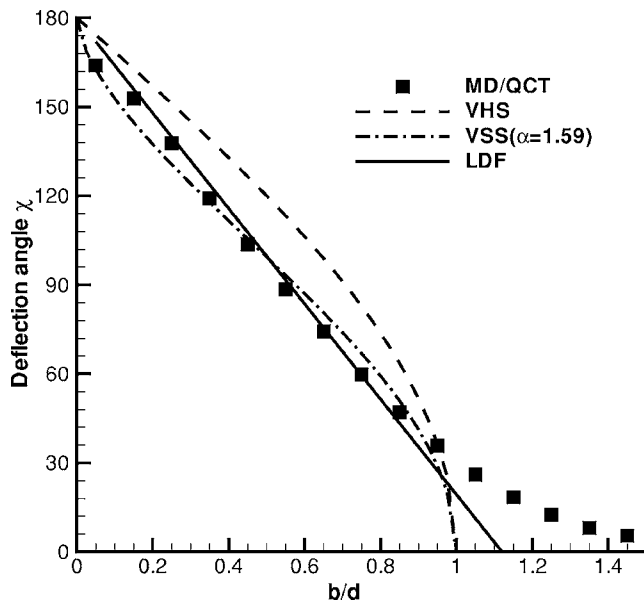


FIG. 4. Comparison of distributions of the deflection angle  $\chi$  for O+HCl collisions predicted by the VHS, VSS, LDF, and MD/QCT. The MD/QCT results were calculated for  $E_{\text{int}}=2.0 \times 10^{-19}$  J and a relative velocity of 5 km/s.

One could also attempt to calculate the total collision cross section for the RP potential surface, but the unbounded nature of a classical total cross section for a realistic potential comes into play. To illustrate, one may use the MD/QCT method to compute

$$\sigma_{\text{VHS}} = \pi b_{\text{max}}^2 \frac{N_c}{N_T}, \quad (8)$$

where  $N_c$  is the number of trajectories that result in a collision and  $N_T$  is the number of total trajectories. However, in order to decide whether a collision has occurred, the cutoff deflection angle,  $\chi$ , is needed, and  $\sigma_{\text{VHS}}$  was found to be strongly dependent on the cutoff angle  $\chi$  for the O+HCl system.

Figure 4 shows a comparison of the distribution of the deflection angle  $\chi$  for O+HCl collisions predicted by the VHS, and variable soft sphere (VSS) (Ref. 14) models, the linear deflection function (LDF), and MD/QCT results. The MD/QCT results were calculated at  $E_{\text{int}}=2.0 \times 10^{-19}$  J and the relative velocity of 5 km/s. This HCl internal energy is typical for the flow field freestream conditions at 120 km and velocity of 5 km/s. For the VHS and VSS models, the deflection functions are given by

$$\chi_{\text{VHS}} = 2 \cos^{-1}(b/d), \quad (9)$$

$$\chi_{\text{VSS}} = 2 \cos^{-1}(b/d)^{1/\alpha}, \quad (10)$$

where  $\alpha$  is an adjustable parameter between 1 and 2, and a value of 1.59 was used in the figure.<sup>5</sup> For this comparison, a diameter,  $d$ , of 2.35 Å was used. The LDF model gives the deflection angle as

$$\chi_{\text{LDF}}(b) = 180(1 - b/d_{\text{LDF}}), \quad (11)$$

where a value of  $d_{\text{LDF}}=2.63$  Å was chosen to match with the MD/QCT results. It is shown that the LDF model agrees better with the MD/QCT results than the VHS and VSS models. However, the discrepancy increases between the MD/QCT results and all of the models for smaller deflection angles. The question of whether the DSMC collision cross sections should be parametrized by the collider pair internal energy has been discussed,<sup>15</sup> but will not be considered here. For higher internal and translational energies, the cutoff angle is more important, and it is difficult to define as may be seen in the figure. Therefore, the approach that Tokumasu<sup>9</sup> used is utilized to calculate the viscosity cross section.

For implementation in DSMC, it is more consistent to obtain a transport-based collision cross section (usually viscosity) from which to convert a reaction cross section to a reaction probability, since the DSMC method already uses the VHS model viscosity-based cross section as the basis for computing the number of collisions per cell per time step and as the basis for collision dynamics (hard-sphere isotropic scattering). In this spirit, the work of Tokumasu and Matsumoto<sup>9</sup> demonstrated the calculation of an accurate viscosity cross section for a given potential using a Monte Carlo method for integration. While the integration over the impact parameter becomes infinite for the total collision cross section, those for classical momentum and energy transfer cross sections are finite. Therefore, the viscosity cross section was calculated first, and converted to the equivalent VHS collision cross section for each collision velocity.<sup>9</sup>

The viscosity cross section,  $\sigma_{\mu}$ , is calculated by the Monte Carlo evaluation of an integral given by Ref. 16

$$\sigma_{\mu, \text{MD}} = \int \left( \frac{\hat{g}^4}{4} \sin^2 \chi + \frac{1}{3} (\Delta \hat{e}_{\text{int}})^2 - \frac{1}{2} (\Delta \hat{e}_{\text{int}})^2 \sin^2 \chi \right) d\tau, \quad (12)$$

where  $\hat{g}$  is the dimensionless relative velocity that is defined as  $\sqrt{m_r/kT}g$ ,  $\hat{e}_{\text{int}}$  is the dimensionless internal energy that is nondimensionalized by  $kT$ , and  $\Delta \hat{e}_{\text{int}}$  is the change of the dimensionless HCl internal energy before and after a collision. The quantities  $\chi$ ,  $\hat{g}$ , and  $\Delta \hat{e}_{\text{int}}$  are obtained from the MD/QCT calculations similar to those performed for the reaction probability except that the sampling of initial trajectory conditions corresponds to the geometric precollisional conditions specified by  $\Delta \hat{e}_{\text{int}}$ . The MD/QCT viscosity cross section  $\sigma_{\mu, \text{MD}}$  converges when the maximum impact parameter is selected so that the effect of the interaction potential is negligible. The integral  $\int()d\tau$  specifies

$$\int()d\tau = \int_0^{b_{\text{max}}} \int_0^\pi \int_0^{2\pi} \int_0^\pi () \left[ \frac{d\psi}{\pi} \right] \left[ \frac{d\phi}{2\pi} \right] \left[ \frac{1}{2} \sin \chi d\chi \right] \times [2\pi b db], \quad (13)$$

where  $\psi$  is the initial orientation of molecules and  $\phi$  is the initial direction of the rotational vector. In addition, the viscosity coefficient,  $\mu$ , is obtained by<sup>17</sup>

TABLE II. Freestream parameters.

Parameter	120 km
Temperature, K	354
Number density, molecule/m <sup>3</sup>	$4.73 \times 10^{17}$
O <sub>2</sub> mole fraction, %	9
N <sub>2</sub> mole fraction, %	73
O mole fraction, %	18

$$\frac{1}{\mu} = \frac{8}{5\sqrt{2\pi m_r kT}} \frac{1}{Q_{\text{int}}} \int_0^\infty dv \int_0^\infty dJ \times \int_0^\infty dE_{\text{tr}} \sigma_\mu \frac{E_{\text{tr}}}{2kT} (2J+1) \exp\left(-\frac{E_{\text{tr}}}{kT} - \frac{E_{\text{vJ}}}{kT}\right), \quad (14)$$

where  $Q_{\text{int}}$  is the partition function for internal modes. The equivalent VHS collision cross section is  $\sigma_{\text{VHS,MD}} = \pi d_{\text{VHS}}^2$ , and the diameter for the collision cross section can be obtained by

$$d_{\text{VHS}} = \sqrt{\frac{6\sigma_{\mu,\text{MD}}}{\pi g^4}}. \quad (15)$$

#### IV. DSMC MODELS, NUMERICAL PARAMETERS, AND FREESTREAM CONDITIONS

Figure 1 shows the flow geometry used in the modeling of the interaction of the atmosphere and the RCS jet. A small rocket is modeled as a blunted cone cylinder and a thruster positioned on the cylinder right after the cone-cylinder junction. The radius of the cylinder is 0.2 m, the length from the head of the cone to the nozzle exit is 2 m, and the angle of attack is zero. The freestream parameters at 120 km altitude are listed in Table II. The species mole fractions at the nozzle exit is also listed in Table III. A starting surface was obtained from the axisymmetric plume core-flow DSMC simulations. The plume core-flow DSMC simulations were performed with the nonuniform nozzle exit condition.<sup>3,4</sup> The density isolines of about  $6 \times 10^{21}$  molecules/m<sup>3</sup> were taken for the starting surface of a 60 lbf (270 N) thruster. The starting surface is an oval shape with approximate  $x$  and  $y$  dimensions of 0.3 and 0.5 m.

The entire set of the chemical reactions between the thruster side jet and plume-atmospheric species includes reactions between oxygen and nitrogen species as well as ones that either produce or consume OH (see Table I). The first

TABLE III. Nozzle exit conditions.

Species	Mole fraction
H <sub>2</sub> O	25%
CO <sub>2</sub>	5%
CO	23%
HCl	14%
N <sub>2</sub>	14%
H <sub>2</sub>	19%

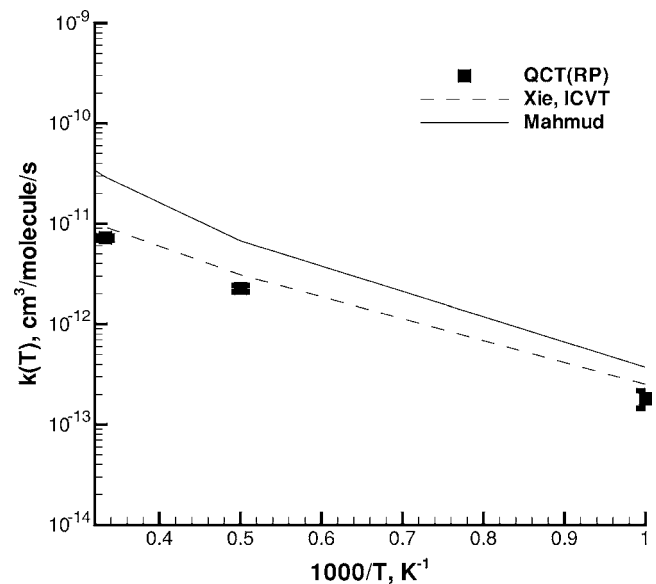


FIG. 5. Reaction rate constant for  $\text{O} + \text{HCl} \rightarrow \text{OH} + \text{Cl}$  as a function of temperature. The MD/QCT(RP) is calculated in this work.

three reactions in Table I involve the dissociation of water by freestream constituents, N<sub>2</sub>, O<sub>2</sub>, and O. Note that the relative importance of these three reactions will change with altitude. The last four reactions are exchange reactions between the freestream and plume constituents. The following two exchange reactions,  $\text{O} + \text{H}_2$  and  $\text{O} + \text{HCl}$ , are potentially important because both H<sub>2</sub> and HCl are present in relatively large mole fractions of divert solid propellant motors.

The three-dimensional DSMC calculations were implemented in the Statistical Modeling In Low-density Environment (SMILE) (Ref. 18) computational tool. The gas is considered a 14-species reacting mixture. Approximately 18 million molecules were simulated in the computational domain. Separate grids were used for collisions and macroparameters adaptive to flow gradients, and the total number of collision cells was approximately 5 million. The total number of time steps was about 100 000 with a time step of  $2.0 \times 10^{-7}$  s, and macroparameter sampling was started after 20 000 time steps, a time sufficient to reach the steady state. These parameters were chosen to minimize the statistical dependence between simulated particles, remove the grid dependence of the results, and furnish sufficient spatial resolution of the boundary layer along the rocket.

The major frequency scheme<sup>18</sup> is employed for modeling the molecular collision frequency to enhance the statistical representation. For trace species, a weighting factor of approximately 0.01 was used. The VHS model was used for modeling nonreactive interactions between particles. The Borgnakke-Larsen<sup>19</sup> (BL) model (see also Ref. 20) with temperature-dependent rotational and vibrational relaxation numbers was chosen for modeling rotation-translation and vibration-translation energy transfer. The effective degree of freedom for vibration was modeled to be temperature-dependent. The gas-surface interaction was modeled using a diffuse model with total energy and momentum accommodation with a surface wall temperature of 300 K.

## V. RESULTS AND DISCUSSION

### A. Rate constant for $\text{O} + \text{HCl} \rightarrow \text{OH} + \text{Cl}$

Although the DSMC method requires the probability of a reaction, instead of the rate constant, the latter quantity provides a consistency check for the MD/QCT calculations presented in this work. Figure 5 presents the reaction rate constant calculated using a parallel MD/QCT code between 1000 K and 3000 K. The reaction rate may be calculated from the reaction cross section by averaging the target molecule (HCl) over a Maxwellian equilibrium distribution,

$$K_f = f(T) Q_{\text{vib}}^{-1} Q_{\text{rot}}^{-1} \left( \frac{8kT}{\pi m_r} \right)^{1/2} \left( \frac{1}{kT} \right)^2 \times \sum_v \sum_J (2J+1) \int_0^\infty \int_0^{b_{\text{max}}} P_r(v, J, E_{\text{tr}}, b) \times \exp(-E_{\text{tr}}/kT) 2\pi b db E_{\text{tr}} dE_{\text{tr}}, \quad (16)$$

where  $Q_{\text{vib}}$  and  $Q_{\text{rot}}$  are the vibrational and rotational partition function, respectively, and for  $\text{O} + \text{HCl}$ ,

$$f(T) = \frac{3}{5 + 3 \exp(-228/T) + \exp(-326/T)}. \quad (17)$$

The factor  $f(T)$  is the probability that the target molecular system is initially on one of the three electronic surfaces that allow a reaction to occur. This temperature dependent expression accounts for the spin-orbit splitting of the overall triplet reagents. The typical number of trajectories per temperature value was approximately 20 000. Figure 5 shows that the rate of Mahmud *et al.*<sup>7</sup> used in our previous DSMC calculations is higher than the MD/QCT(RP) rate obtained with the RP surface in this work and the improved canonical variational theory (ICVT) rate constant of Xie *et al.*<sup>10</sup> The MD/QCT(RP) rate is slightly lower than the ICVT rate because only the  $^3A''$  surface was used for MD/QCT calculations, and the  $^3A'$  surface contribution increases for higher temperature. In addition, the tunneling effect, not included in the MD/QCT calculations, is more important for lower temperatures.

### B. Reaction probability for $\text{O} + \text{HCl} \rightarrow \text{OH} + \text{Cl}$

Figure 6 shows a comparison of reaction probabilities between the MD/QCT and TCE (Ref. 6) models as a function of reactant internal energy at 3 and 5 km/s relative velocities. The MD/QCT reaction probability is calculated here as the reaction cross section divided by the VHS cross section using Bird's values.<sup>5</sup> The rate of Mahmud *et al.*<sup>7</sup> used for our previous simulations and the rate of Xie *et al.*<sup>10</sup> are also shown in the figure. The effective number of degrees of freedom for vibration  $\zeta_{v,\text{HCl}} = 1$  is used, and the VHS model with the parameters of Ref. 5 of  $\omega = 0.375$ ,  $d_{\text{ref}} = 4.38 \text{ \AA}$ , and  $T_{\text{ref}} = 273 \text{ K}$  was used for all the three cases in this subsection. In the next subsection, the fidelity of these-specific VHS values used will be discussed. It can be seen that the TCE probabilities computed from the rate of Mahmud *et al.*<sup>7</sup> are much higher than the MD/QCT or TCE model using the Arrhenius parameters derived from the rate coefficients computed by Xie *et al.*<sup>10</sup> for both relative velocities. This result is con-

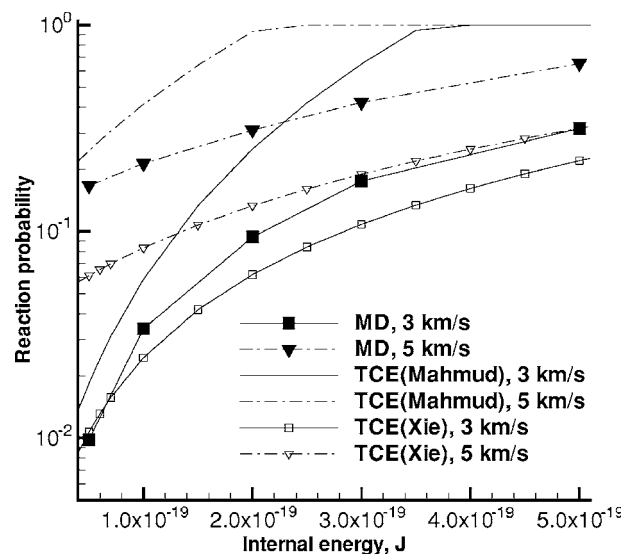


FIG. 6. Comparison between MD/QCT and TCE models: Reaction probabilities for  $\text{O} + \text{HCl} \rightarrow \text{OH} + \text{Cl}$  as a function of the reactant internal energy.

tent with our previous calculations in which the probabilities for the  $\text{O} + \text{HCl}$  reaction, using the TCE model and Mahmud extrapolated rates, were found to be unrealistically high. For the 3 km/s case, the MD/QCT model predicts slightly higher reaction probabilities than the TCE with the rate calculations of Xie *et al.*<sup>10</sup> Nonetheless, at 5 km/s, the discrepancy becomes more significant, and the MD/QCT model predicts higher probabilities than the TCE model.

### C. Collision cross section for $\text{O} + \text{HCl}$

In the previous subsection, the VHS collision cross section with  $\omega = 0.375$ ,  $d_{\text{ref}} = 4.38 \text{ \AA}$  and  $T_{\text{ref}} = 273 \text{ K}$  was used. In this subsection, the preferred values for VHS for  $\text{O} + \text{HCl}$  collisions is investigated. In our earlier reported results,<sup>3,4</sup> the viscosity index  $\omega$  of 0.25 for O and  $\omega$  of 0.5 for HCl were used,<sup>5,21</sup> i.e., the HCl molecule was treated in the Maxwell model. However, although the viscosity index  $\omega$  of HCl is 0.5 between 20 and 99 °C, for some gases,  $\omega$  decreases as temperature increases.<sup>21</sup> Therefore, the VHS collision cross sections obtained from a Maxwell molecule may not be accurate for higher temperatures.

Let us consider the selection of two parameters: (1) temperature exponent of the viscosity coefficient,  $\nu$ , and (2) the reference diameter,  $d_{\text{ref}}$ , for the VHS model. The parameters used in the previous DSMC calculations were mostly obtained from viscosity data in the low temperature range.<sup>21</sup> Figure 7 shows the variation of viscosity coefficient of HCl from 100 to 5000 K. In the figure, the data of Svehla<sup>22</sup> and the data (Bird) in Ref. 21 are shown. Svehla estimated the viscosities using the Lennard-Jones (12-6) potentials. From the data (Bird), the temperature exponent of the viscosity coefficient of HCl,  $\nu_{\text{HCl}}$ , is 1.0, and with  $\nu_{\text{HCl}}$  of 1.0, the viscosity coefficient is higher than the data of Svehla. The temperature exponent of the viscosity coefficient of HCl,  $\nu_{\text{HCl}}$ , of 0.65 agrees well with the data of Svehla between



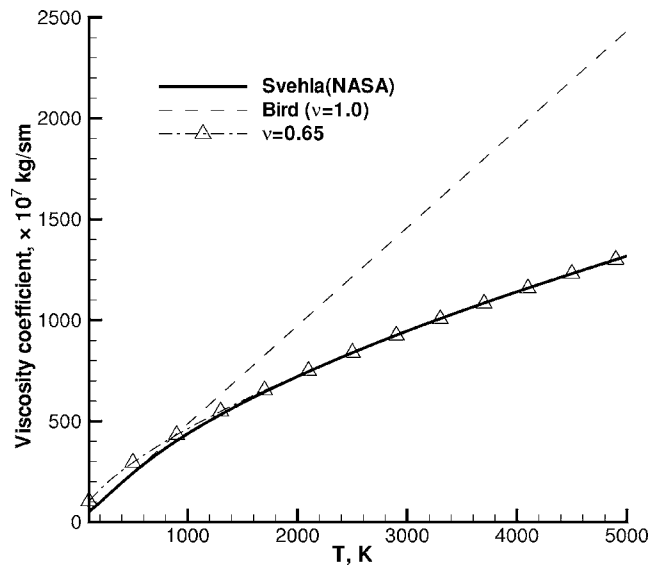


FIG. 7. HCl viscosity coefficient,  $\mu$ , for high temperatures. Svehla's viscosity coefficient is compared with the Maxwell model (Bird,  $\nu=1.0$ ).  $\nu_{\text{HCl}}$  of 0.65 gives great agreement with the data of Svehla.

1000 and 5000 K. The VHS parameters for HCl are listed in Table IV. It is seen that the value of  $\omega$  is quite different for low and high temperatures.

Using the RP  $^3A''$  surface in the MD/QCT calculations, the quantities such as deflection angle and the change in HCl internal energy are obtained and used in Eq. (12) to calculate the viscosity cross section. The change in HCl internal energy,  $\hat{e}_{\text{int}}$ , is obtained by analyzing the momentum of the postcollisional HCl species in each trajectory. To account for the neglect of the RP  $^3A''$  potential, the maximum impact parameter was selected such that the rate of translational energy transfer was less than 10%, and the MD/QCT viscosity cross section  $\sigma_{\mu,\text{MD}}$  converged. The approach that Tokumasu used is this work to obtain both the O+HCl viscosity coefficients as well as the VHS-equivalent collision cross section.

Figure 8 shows a comparison of the viscosity coefficients obtained from the MD/QCT results and the O and HCl data in Ref. 21 (Bird) and data of Svehla.<sup>22</sup> To compare with the MD/QCT result we take the average of the separate O and HCl viscosity coefficients. The MD/QCT results for O+HCl are believed to be the most accurate and fall above or below the data of Refs. 21 (Bird) and 22, depending on the temperature. The agreement between the MD/QCT results and the viscosities derived from the low-temperature data of Ref. 21 is good. At higher temperatures, the difference in the MD/QCT results and the viscosities derived from the coefficients of Svehla is attributed to the simpler potential model used in the latter calculations.

Figure 9 presents a comparison of the collision cross

TABLE IV. VHS parameters for HCl.

Data	$\omega$	$d_{\text{ref}}, \text{\AA}$	$T_{\text{ref}}, \text{K}$
Bird	0.50	5.76	273
Svehla	0.15	3.15	5000

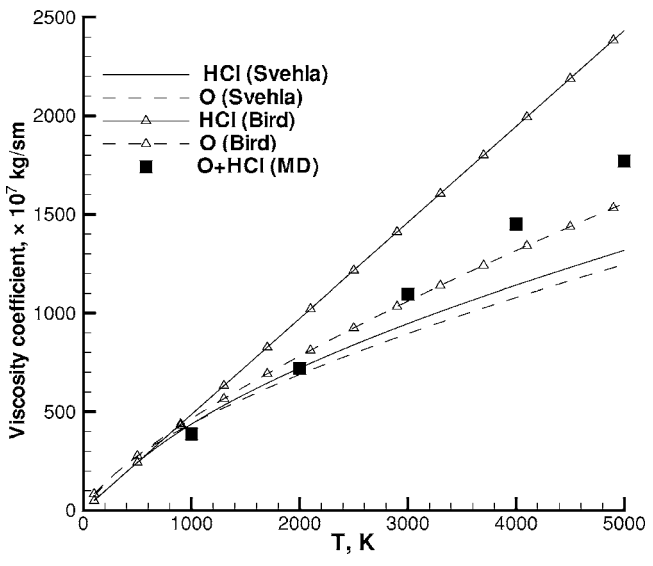


FIG. 8. O and HCl mixture viscosity for high temperatures calculated by the MD/QCT method [Eq. (14)].

sections between the MD/QCT and VHS models at  $E_{\text{int}} = 0.5 \times 10^{-19}$  and  $2.0 \times 10^{-19}$  J. For the two viscosity parameters tested in the VHS model, Fig. 9 shows that the collision cross sections are greater with high temperature data of Svehla.<sup>22</sup> The VHS cross section with  $\omega_{\text{HCl}}=0.15$  and  $d_{\text{HCl,ref}}=3.15$  at 5000 K (Svehla) is significantly larger than the VHS cross section with  $\omega_{\text{HCl}}=0.5$  and  $d_{\text{HCl,ref}}=5.76$  at 273 K (Bird) by more than 50%. The MD/QCT results are between the VHS cross sections obtained from the data of Ref. 5 (Bird) and those of Svehla.<sup>22</sup> Therefore, if the MD/QCT VHS equivalent collision cross section in Eq. (15) is used, lower reaction probabilities are predicted than those that would be obtained from the VHS cross sections using the data in Ref. 5 (Bird). Also, it was found that the MD/QCT VHS equivalent cross section does not change sig-

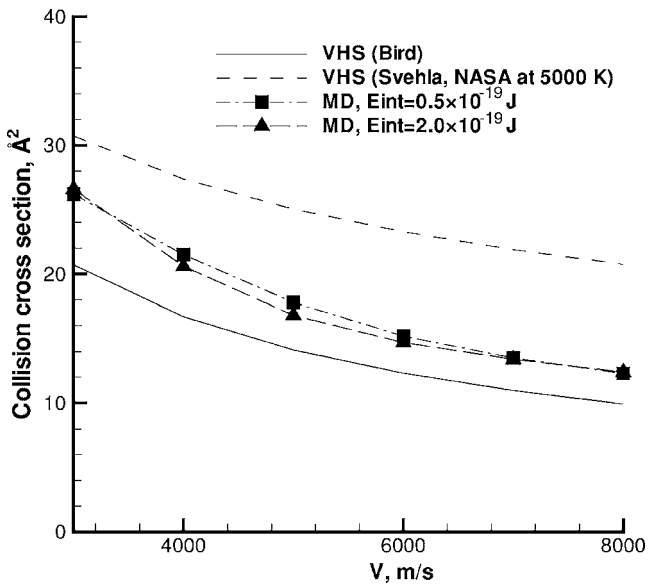


FIG. 9. Comparison of collision cross sections between MD/QCT and VHS models for the O+HCl collision.

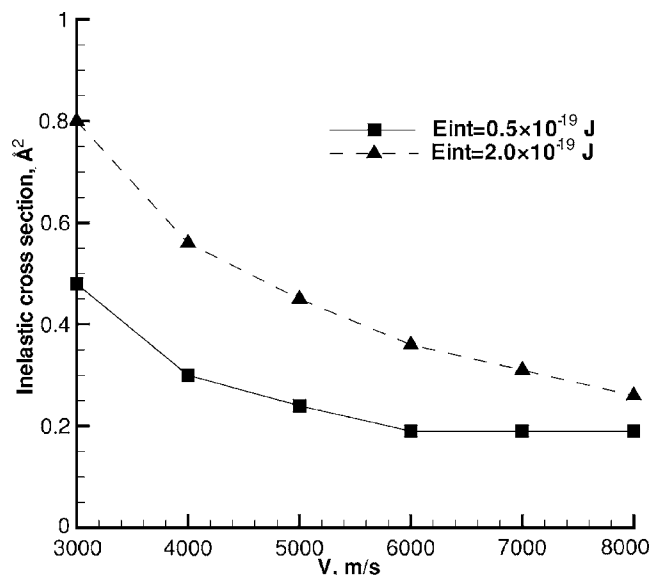


FIG. 10. Comparison of inelastic collision cross sections for the O+HCl collision at  $E_{\text{int}}=0.5 \times 10^{-19}$  and  $E_{\text{int}}=2.0 \times 10^{-19}$  J.

nificantly with changes of the HCl internal energy. Since the MD/QCT VHS equivalent cross section is not dependent on the HCl internal energy, the cross sections could be fit to the simpler VHS model. The parameters,  $\omega=0.39$  and  $d_{\text{ref},1000\text{ K}}=3.9 \text{ \AA}$  were found to give a good fit of the MD/QCT cross sections to the VHS form. The collision cross sections derived from these parameters will be designated as  $\sigma_{\text{VHS,MD}}$ .

The inelastic collision cross section,  $\sigma_{\text{in}}$ , is defined for collisions that do not react but produce a change in  $E_{\text{tr}}$  as

$$\sigma_{\text{in}} = \int (\Delta \hat{e}_{\text{tr}})^2 d\tau. \quad (18)$$

The quantity  $\Delta \hat{e}_{\text{tr}}$  is the change of the dimensionless translational energy before and after a collision and was calculated from the MD/QCT pre and post trajectory HCl conjugate momenta for nonreactive trajectories as

$$\Delta \hat{e}_{\text{tr}} = \frac{\hat{g}'^2}{2} + \hat{e}_{\text{CM}} - \frac{\hat{g}^2}{2} \quad (19)$$

where  $\hat{e}_{\text{CM}}$  is the dimensionless center-of-mass translational energy, and the prime indicates postcollisional quantities. Figure 10 shows the inelastic collision cross section as a function of the relative velocity. As shown in the figure, the inelastic cross section decreases as the translational energy increases. It is also found that the inelastic cross section is a function of both the translational and internal energy. However, because the change of  $\sigma_{\text{in}}$  is insignificant compared to the VHS-equivalent collision cross section,  $\sigma_{\text{VHS,MD}}$  does not show a strong dependence on internal energy.

Figures 11 and 12 show a comparison of the reaction probability for  $\text{O} + \text{HCl} \rightarrow \text{OH} + \text{Cl}$  calculated by using the reaction cross section divided by either the VHS model (Bird) or  $\sigma_{\text{VHS,MD}}$  at 3 km/s and 5 km/s, respectively. The VHS model with  $\omega=0.39$  and  $d_{\text{ref},1000\text{ K}}=3.9 \text{ \AA}$  was used to represent  $\sigma_{\text{VHS,MD}}$  because the MD/QCT collision cross section

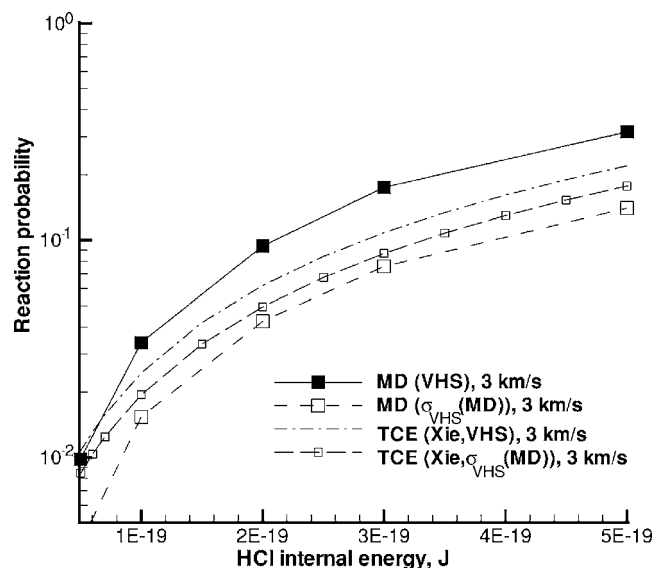


FIG. 11. Comparison of the reaction probability calculated by using the reaction cross section divided by either the VHS model (Bird) or the MD/QCT collision cross section ( $\sigma_{\text{VHS,MD}}$ ): Reaction probabilities as a function of the reactant internal energy at 3 km/s.

results agree well with the VHS model with those parameters as shown in Fig. 9. Both the MD/QCT and TCE reaction probabilities using  $\sigma_{\text{VHS,MD}}$  are lower than those with the VHS cross section (Bird,  $\omega_{\text{HCl}}=0.5$ ) because  $\sigma_{\text{VHS,MD}}$  are greater than the VHS cross sections (Bird,  $\omega_{\text{HCl}}=0.5$ ). However, the change in the TCE model is smaller than that in the MD/QCT model.

Figure 13 shows computed MD/QCT reaction probability values (using  $\sigma_{\text{VHS,MD}}$ ) as a function of total collision energies. The filled and open symbols show the reaction probabilities for a given collision velocity with varying internal energy and with a fixed internal energy with varying collision velocity, respectively. The results show no significant favoring effect of internal energy on the reaction prob-

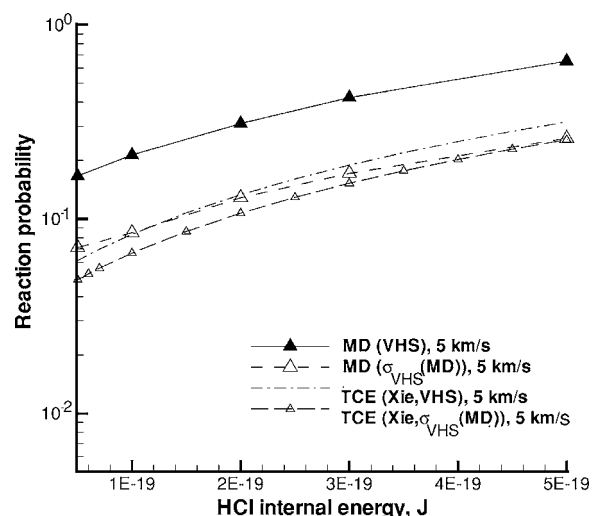


FIG. 12. Comparison of the reaction probability calculated by using the reaction cross section divided by either the VHS model (Bird) or the MD/QCT collision cross section ( $\sigma_{\text{VHS,MD}}$ ): Reaction probabilities as a function of the reactant internal energy at 5 km/s.

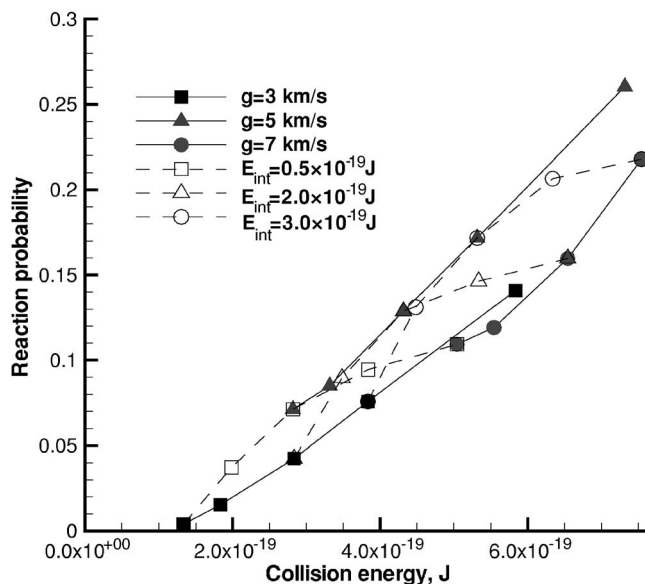


FIG. 13. Reaction probability as a function of total collision energy for different collision velocities and HCl internal energies. Note that 3, 5, 7 km/s corresponds to  $8.3 \times 10^{-20}$ ,  $2.3 \times 10^{-19}$ ,  $4.5 \times 10^{-19}$  J, respectively.

ability. This result is somewhat surprising in that Aoiz *et al.*<sup>23</sup> found significant vibrational favoring effects in their QCT results for this reaction. However a less accurate PES was used in that study.

Figure 14 presents the distributions of the  $\Delta\hat{e}_{\text{int}}$  at 5 km/s for O+HCl collision for two initial internal energies.  $\Delta\hat{e}_{\text{int}}$  was calculated by  $\Delta\hat{e}_{\text{int}} = \hat{e}'_{\text{int}} - \hat{e}_{\text{int}}$ . Figure 14 shows that as the initial HCl internal energy increases, the  $\Delta\hat{e}_{\text{int}}$  distribution spreads. In other words, the inelastic cross section increases, as the initial internal energy increases, as is generally expected based on simple models (see, e.g., Ref. 24). At  $E_{\text{int}} = 0.5 \times 10^{-19}$  J, energy is mostly transferred from the translational to HCl internal modes. Figure 15 shows the distributions of the  $\Delta\hat{e}_{\text{int}}$  at  $E_{\text{int}} = 2.0 \times 10^{-19}$  J for different

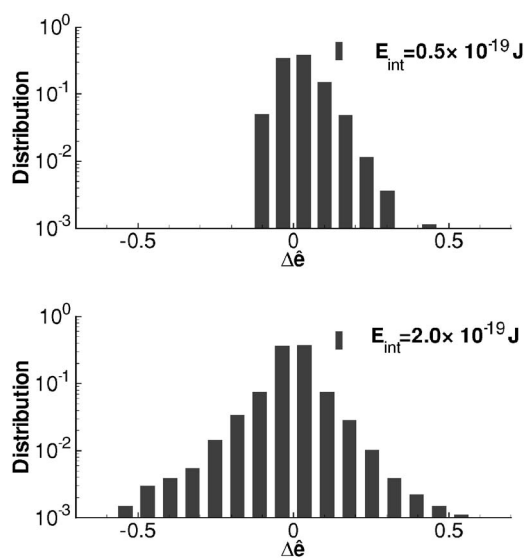


FIG. 14. Distribution of the  $\Delta\hat{e}_{\text{int}}$  for  $E_{\text{int}} = 0.5 \times 10^{-19}$  J (top) and  $E_{\text{int}} = 2.0 \times 10^{-19}$  J (bottom) at 5 km/s for the O+HCl collision.

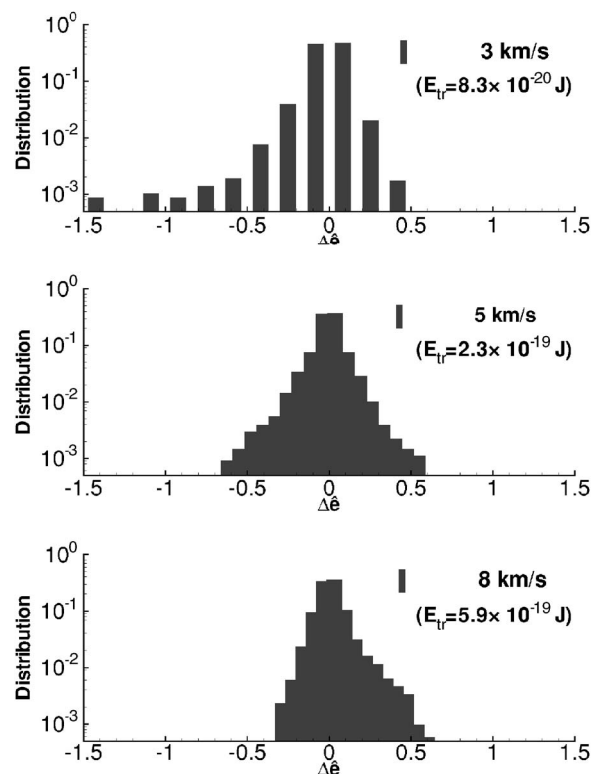


FIG. 15. Distribution of the  $\Delta\hat{e}_{\text{int}}$  for  $E_{\text{int}} = 2.0 \times 10^{-19}$  J at 3 km/s (top), 5 km/s (middle), and 8 km/s (bottom) for the O+HCl collision.

collisional translational energies. At 3 km/s, the energy is transferred from the HCl internal to the translational mode. However, as the initial translational energy increases, the energy shifts from the translational to internal modes. In general the results show a tendency toward energy equilibration between modes. When  $E_{\text{tr}} > E_{\text{int}}$ , the  $E_{\text{int}}$  gains and when  $E_{\text{int}} > E_{\text{tr}}$ , the  $E_{\text{tr}}$  gains.

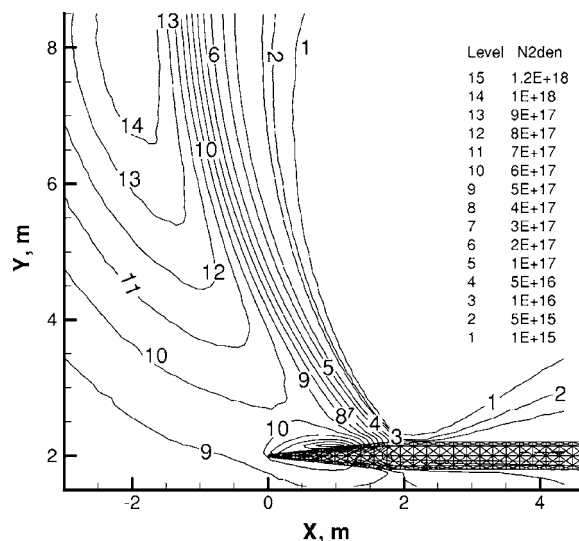


FIG. 16. N<sub>2</sub> number density (molecule/m<sup>3</sup>) contours with the rate of Xie *et al.* (TCE) at 120 km altitude for freestream velocity of 5 km/s. Area shown is  $7.4 \times 7.5$  m.

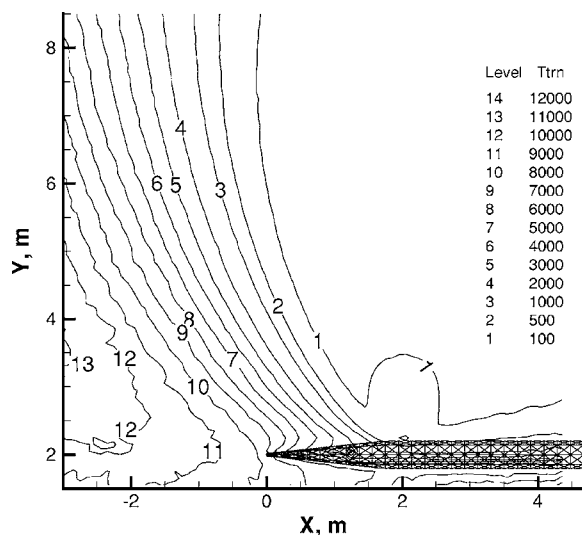


FIG. 17. Translational temperature contours with the rate of Xie *et al.* (TCE) at 120 km altitude for freestream velocity of 5 km/s. Area shown is  $7.4 \times 7.5$  m.

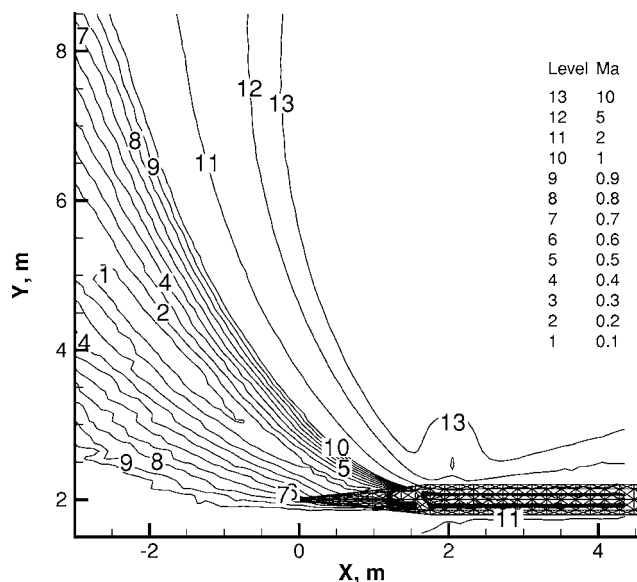


FIG. 18. Mach number contours with the rate of Xie *et al.* (TCE) at 120 km altitude for freestream velocity of 5 km/s. Area shown is  $7.4 \times 7.5$  m.

#### D. DSMC calculations

First, the TCE model with the rate constant of Xie *et al.*<sup>10</sup> for the  $O+HCl \rightarrow OH+Cl$  reaction was utilized for the DSMC calculation at 120 km altitude for freestream velocity of 5 km/s. For the TCE model, the VHS collision cross section for  $O+HCl$  with  $\omega=0.375$ ,  $d_{ref}=4.38$  Å and  $T_{ref}=273$  K was used. Figure 16 shows the  $N_2$  number density (molecule/ $m^3$ ) contour for this case. The maximum  $N_2$  number density is about  $1.2 \times 10^{18} m^{-3}$  located at 1–2 m ahead of the rocket cone. It was found that the change of chemical reaction models and  $O+HCl$  collision cross section do not affect the overall flow field because collisions between O and HCl are not the main collision pairs (O is 18% of the freestream and HCl is 14% of the side jet). Figure 17 shows the overall translational temperature contour with the rate constant of Xie *et al.* for the  $O+HCl \rightarrow OH+Cl$  reaction at 120 km altitude for freestream velocity of 5 km/s. Similar to the total number density, the overall translational temperature profile does not change for the different  $O+HCl$  reaction probabilities. While the high number density shock region is located between  $x=-2$  and  $-1$  m, the high temperature shock region is shifted more forward than the high number density shock region. Figure 18 shows the Mach number contours at 120 km altitude for a freestream velocity of 5 km/s. The high temperature shock region coincides with the low Mach number region.

Second, the DSMC calculations were implemented for the three  $O+HCl$  chemical reaction models at 120 km altitude for freestream velocity of 5 km/s. In the discussion below, we designate the TCE model used with the previous rate constant<sup>7</sup> as case (1); the TCE model using the rate constant of Xie *et al.*<sup>10</sup> as case (2); and, the MD/QCT reaction probability as case (3). For case (3), the MD/QCT reaction probability used in this subsection is the ratio of the MD/QCT reaction cross section to the  $\sigma_{VHS,MD}$ , and the computed MD/QCT reaction probabilities were tabulated and used in the DSMC simulations. For cases (1) and (2), the

$O+HCl$  collision cross section used in calculating the elastic cross section for pair-selection and elastic collision outcomes was the VHS model with the original parameters of  $\omega=0.375$  and  $d_{ref,273 K}=4.38$  Å. For case (3), the VHS model with the modified parameters,  $\omega=0.39$  and  $d_{ref,1000 K}=3.9$  Å was used. The change in collision cross sections changes the number of collisions between O and HCl molecules which in turn, affects the OH production rate.

Figure 19 shows the OH number density contours with a maximum OH number density of about  $2 \times 10^{16} m^{-3}$  with the case (2) chemical reaction rate. In Figs. 20 and 21, a quantitative comparison between the three chemical reaction models is shown. Figures 20 and 21 present the OH number density distributions along the  $y=8$  m line and the  $x=-1.5$  m line, respectively. As expected, the TCE model of

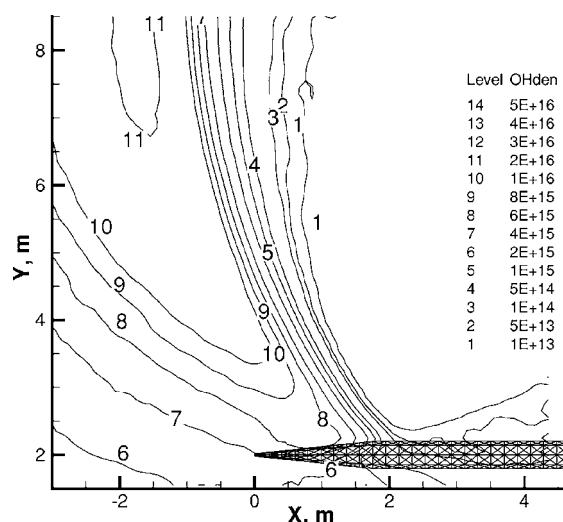


FIG. 19. OH number density (molecule/ $m^3$ ) contours with the rate of Xie *et al.* (TCE) at 120 km altitude for the freestream velocity of 5 km/s. Area shown is  $7.4 \times 7.5$  m.



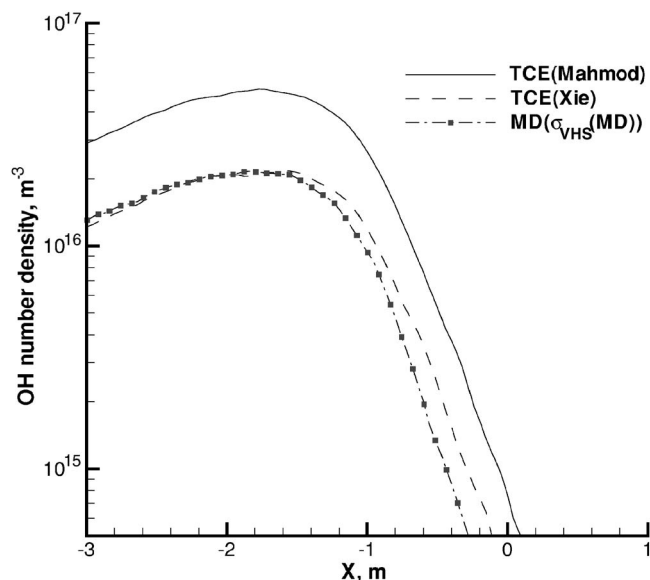


FIG. 20. Comparison of OH number density (molecule/m<sup>3</sup>) at  $y=8$  m for three chemical reaction models at 120 km altitude for the freestream velocity of 5 km/s.

case (1) predicts higher OH production than the MD/QCT model. With the case (1) reaction rate, the OH production was much more than the other two cases (2) and (3) because the  $O+HCl$  reaction probability was significantly higher, as shown in Figs. 2 and 6. With the case (2) reaction rate, the maximum OH number density is reduced by more than 50% whereas with the MD/QCT probability, it is slightly lower than for case (2). There are two factors that caused the change in OH production between case (2) and (3). The first factor is the larger  $O+HCl$  collision cross section obtained by the MD/QCT method that leads to more OH molecules being produced. The second factor is the lower MD/QCT

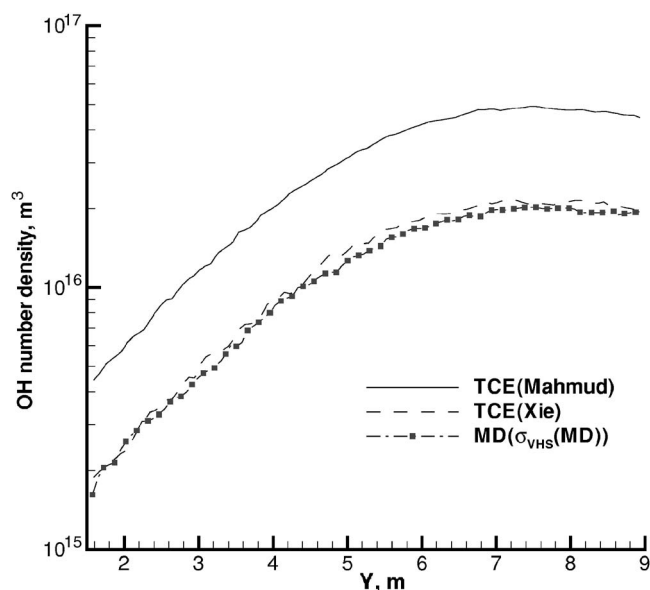


FIG. 21. Comparison of OH number density (molecule/m<sup>3</sup>) at  $x=-1.5$  m for three chemical reaction models at 120 km altitude for the freestream velocity of 5 km/s.

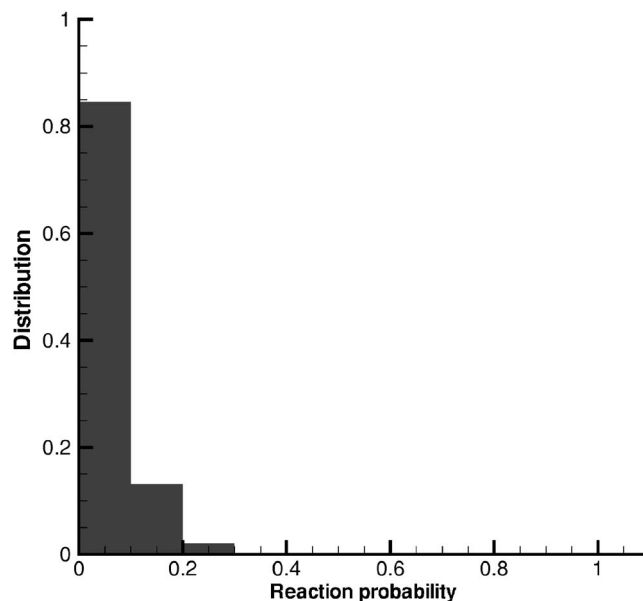


FIG. 22. Reaction probability distribution for  $O+HCl \rightarrow OH+Cl$  using the TCE model (the rate of Xie *et al.*) for an altitude of 120 km and a freestream velocity 5 km/s.

reaction probability, however, the effect of the change of collision cross sections was found to be smaller than the change of reaction probability. Thus, these two factors result in a slightly lower OH number density compared to case (2).

In the shock region, the reaction probabilities changed dramatically between cases (1) and (2). For case (1), the reaction rate results in TCE reaction probabilities greater than one, as cases found in our previous work. (In the DSMC calculation, they are set to one.) Due to the jet-atmosphere interaction, high translational energies result in high reaction probabilities for the TCE model. About 10% of the  $O+HCl$

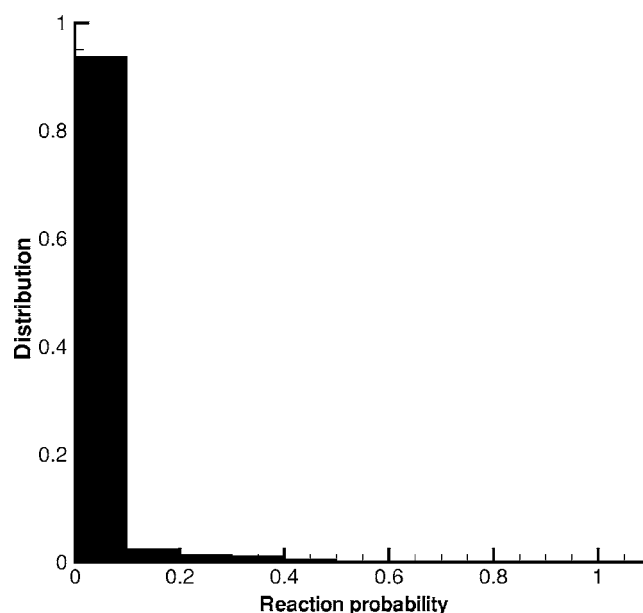


FIG. 23. Reaction probability distribution for  $O+HCl \rightarrow OH+Cl$  using the MD/QCT model for an altitude of 120 km and a freestream velocity of 5 km/s.

collisions results in the probability greater than one with the rate (1) using the TCE model as shown in Fig. 3. In contrast, with the rate of Xie *et al.*, case (2), most of the O+HCl collisions are predicted to have a TCE reaction probability smaller than 0.4 (see Fig. 22). Finally, the reaction probability with the MD/QCT, case (3), is still lower than the other two, and more than 80% of the reaction had the probability of lower than 0.1 as shown in Fig. 23.

Using the same VHS (Bird values) collision cross section for the TCE and MD/QCT reaction models, the MD/QCT predicts higher reaction probability than case (2) as shown in Fig. 6. In contrast, if both the reaction and collision cross sections are obtained by the MD/QCT method, the MD/QCT reaction probability becomes lower than the TCE with the rate (2). At 5 km/s, the MD/QCT and the case (2) TCE reaction probabilities are very close, but at 3 km/s or 8 km/s, the case (2) reaction probability is higher than those obtained with the MD/QCT.

## VI. CONCLUSION

Chemically reacting flows of the interaction of a jet with a transitional-to-rarefied atmosphere have been simulated using the DSMC method. The objective of this work was to assess the sensitivity of the flow modeling to the fidelity of chemical reaction models in hypervelocity collisions in DSMC. The  $O(^3P)+HCl(^1\Sigma^+)\rightarrow OH(^2\Pi)+Cl(^2P)$  chemical reaction was selected for study since it is an important reaction path in atmospheric-jet interaction flows. The MD/QCT calculations were performed for the O+HCl reaction using the *ab initio*  $^3A''$  potential energy surface of Ramachandran and Peterson (RP) (Ref. 8) for both reaction and collision cross sections. The approach of Tokumasu was utilized to calculate the viscosity cross sections, and the VHS-equivalent collision cross sections were obtained with the assumption of isotropic scattering. Finally, the MD/QCT reaction probabilities were compared with those obtained by the TCE model with two rates.

These results show that using the same VHS collision cross section, the MD/QCT reaction probability was predicted to be lower than the TCE probability with the rate of Mahmud *et al.*<sup>7</sup> used in Ref. 3 (1) and higher than the TCE probability with the rate of Xie *et al.*<sup>10</sup> (2). The TCE model with rate (1) predicted reaction probabilities higher than one in the energy range of interest. The VHS cross section was found to be very sensitive to the viscosity parameters, obviously. Therefore, to be accurate, the MD/QCT collision cross sections using the approach that Tokumasu used were calculated for the range of relative velocities and internal energies of interest.

The energy transfer between the translational and internal modes was also investigated. For the initial HCl internal energy of  $5 \times 10^{-20}$  J, translational energy was transferred to the HCl internal modes. The average of energy shift, however, was found to be almost zero for an initial HCl internal energy of  $2 \times 10^{-19}$  J. The magnitude of the inelastic cross sections is small compared to the total cross section. The dependence on the initial internal energy is so small that the MD/QCT VHS equivalent collision cross sections were con-

verted to fit the VHS with  $\omega=0.39$  and  $d_{ref}=3.9$  at 1000 K. These values were used for the MD/QCT reaction probabilities, and these probabilities were tabulated and used in DSMC.

The DSMC simulations were performed for the atmosphere-jet interaction flows for an altitude of 120 km, a freestream velocity 5 km/s, and three O+HCl chemical reaction models. The chemical reaction models did not affect the overall flow field, but affected the properties of the product species, OH. Although the TCE with rate (1) resulted in a reaction probability higher than one, the TCE with rate (2) and MD/QCT models showed that the O+HCl reaction has a maximum probability less than 0.4. Also, the OH production was slightly lower with the MD/QCT than the TCE rate (2) model.

For low enthalpy reactions, in hypervelocity collisions, the TCE model with accurate Arrhenius rates appears to agree well with rigorous MD/QCT calculations. Good agreement between TCE and MD/QCT is observed because this reaction does not show strong favoring. However, in the regime where the TCE reaction probability approaches unity, one should verify the total collision cross section.

*Note added in proof.* A very recent work by Camden and Schatz<sup>25</sup> provides important new direct dynamics results on the reaction cross sections for O+HCl.

## ACKNOWLEDGMENTS

The research performed at the Pennsylvania State University was supported by the Air Force Office of Scientific Research Grant No. F49620-02-1-0104, and the work performed at Edwards AFB was supported by the U.S. Air Force Office of Scientific Research, both efforts administered by Dr. Mitat Birkan. We would also like to acknowledge support from the Missile Defense Agency MSTAR program, Contract No. HQ0006-05-C-0021. Special thanks are to Dr. Sergey Gimelshein for discussing the details of the calculations and to Dr. L. S. Bernstein and Dr. W. L. Dimpfl for the use of the LDF model.

<sup>1</sup>J. D. Anderson, in *Hypersonic and High-Temperature Gas Dynamics*, 2nd ed. (AIAA, Reston, 2006).

<sup>2</sup>T. Ozawa, D. Fedosov, D. A. Levin, and S. F. Gimelshein, "Quasiclassical trajectory modeling of OH production in direct simulation Monte Carlo," *J. Thermophys. Heat Transfer* **19**, 235 (2005).

<sup>3</sup>S. F. Gimelshein, D. A. Levin, and A. A. Alexeenko, "Modeling of the chemically reacting flows from a side jet at high altitudes," *J. Spacecr. Rockets* **41**, 582 (2004).

<sup>4</sup>S. F. Gimelshein, A. A. Alexeenko, and D. A. Levin, "Modeling of the interaction of a side jet with a rarefied atmosphere," *J. Spacecr. Rockets* **39**, 168 (2002).

<sup>5</sup>G. A. Bird, in *Molecular Gas Dynamics and the Direct Simulation of Gas Flows* (Clarendon, Oxford, 1994).

<sup>6</sup>G. A. Bird, in *Rarefied Gas Dynamics*, edited by S. Fisher (AIAA, New York, 1981), Vol. 74, pp. 239–255.

<sup>7</sup>K. Mahmud, J.-S. Kim, and A. Fontijn, "A high-temperature photochemical kinetics study of the O+HCl reaction from 350 to 1480 K," *J. Phys. Chem.* **94**, 2994 (1990).

<sup>8</sup>B. Ramachandran and K. A. Peterson, "Potential energy surfaces for the  $^3A''$  and  $^3A'$  electronic states of the  $O(^3P)+HCl$  system," *J. Chem. Phys.* **119**, 9590 (2003).

<sup>9</sup>T. Tokumasu and Y. Matsumoto, "Dynamic molecular collision (DMC) model for rarefied gas flow simulations by the DSMC method," *Phys. Fluids* **11**, 1907 (1999).

- <sup>10</sup>T. Xie, J. M. Bowman, K. A. Peterson, and B. Ramachandran, "Quantum calculations of the rate constant for the  $O(^3P)HCl$  reaction on new *ab initio*  $^3A''$  and  $^3A'$  surfaces," *J. Chem. Phys.* **119**, 9601 (2003).
- <sup>11</sup>A. J. C. Varandas, J. Brando, and M. R. Pastrana, "Quasiclassical trajectory calculations of the thermal rate coefficients for the reactions  $H(D) + O_2 \rightarrow OH(D) + O$  and  $O + OH(D) \rightarrow O_2 + H(D)$  as a function of temperature," *J. Chem. Phys.* **96**, 5137 (1992).
- <sup>12</sup>T. Xie, J. Bowman, J. W. Duff, M. Braunstein, and B. Ramachandran, "Quantum and quasiclassical studies of the  $O(^3P) + HCl \rightarrow OH + Cl(^2P)$  reaction using benchmark potential surfaces," *J. Chem. Phys.* **122**, 014301 (2005).
- <sup>13</sup>E. S. Severin, B. C. Freasier, N. D. Hamer, D. L. Jolly, and S. Nordholm, "An efficient microcanonical sampling method," *Chem. Phys. Lett.* **57**, 117 (1978).
- <sup>14</sup>K. Koura and H. Matsumoto, "Variable soft sphere molecular model for inverse-power-law or Lennard-Jones potential," *Phys. Fluids A* **3**, 2459 (1991).
- <sup>15</sup>I. J. Wysong, in *Rarefied Gas Dynamics*, edited by R. Brun, R. Campargue, R. Gatignol, and J. C. Lengrand (AIAA, Marseille, 1998), Vol. 2, pp. 3–14.
- <sup>16</sup>J. A. Lordi and R. E. Mates, "Rotational relaxation in nonpolar diatomic gases," *Phys. Fluids* **13**, 291 (1970).
- <sup>17</sup>N. Taxman, "Classical theory of transport phenomena in dilute polyatomic gases," *Phys. Rev.* **110**, 1235 (1958).
- <sup>18</sup>M. S. Ivanov and S. V. Rogasinsky, "Analysis of the numerical techniques of the direct simulation Monte Carlo method in the rarefied gas dynamics," *IMA J. Numer. Anal.* **3**, 453 (1988).
- <sup>19</sup>C. Borgnakke and P. S. Larsen, "Statistical collision model for Monte Carlo simulation of polyatomic gas mixture," *J. Comput. Phys.* **18**, 405 (1975).
- <sup>20</sup>I. D. Boyd, "Relaxation of discrete rotational energy distributions using a Monte Carlo method," *Phys. Fluids A* **5**, 2278 (1993).
- <sup>21</sup>S. Chapman and T. G. Cowling, in *The Mathematical Theory of Non-Uniform Gases*, 3rd ed. (Cambridge University Press, New York, 1970), Chap. 12.
- <sup>22</sup>R. A. Svehla, "Estimated viscosities and thermal conductivities of gases at high temperatures," NASA TR R-132 (1962).
- <sup>23</sup>F. J. Aoiz, L. Bnares, J. F. Castillo, M. Menendez, and J. E. Verdasco, "Quantum mechanical and quasi-classical rate constant calculations for the  $O(^3P) + HCl \rightarrow OH + Cl$  reaction," *Phys. Chem. Chem. Phys.* **1**, 1149 (1999).
- <sup>24</sup>R. N. Schwartz, Z. I. Slawsky, and K. F. Herzfeld, "Calculation of vibrational relaxation times in gases," *J. Chem. Phys.* **20**, 1591 (1952).
- <sup>25</sup>J. P. Camden and G. C. Schatz, "Direct dynamics simulations of  $O(^3P) + HCl$  at hyperthermal collision energies," *J. Phys. Chem. A* **110**, 13681 (2006).